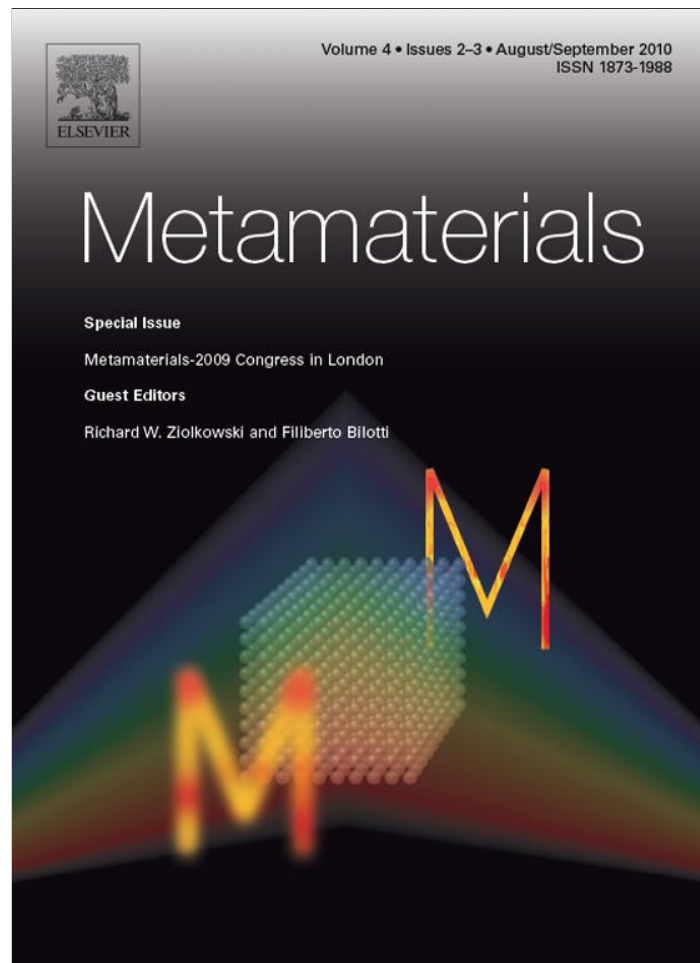


Provided for non-commercial research and education use.  
Not for reproduction, distribution or commercial use.



This article appeared in a journal published by Elsevier. The attached copy is furnished to the author for internal non-commercial research and education use, including for instruction at the authors institution and sharing with colleagues.

Other uses, including reproduction and distribution, or selling or licensing copies, or posting to personal, institutional or third party websites are prohibited.

In most cases authors are permitted to post their version of the article (e.g. in Word or Tex form) to their personal website or institutional repository. Authors requiring further information regarding Elsevier's archiving and manuscript policies are encouraged to visit:

<http://www.elsevier.com/copyright>



## Fresh metamaterials ideas for metallic lenses

M. Navarro-Cía<sup>a</sup>, M. Beruete<sup>a</sup>, I. Campillo<sup>b</sup>, M. Sorolla<sup>a,\*</sup>

<sup>a</sup> Millimeter and Terahertz Waves Laboratory, Universidad Pública de Navarra, Campus Arrosadía, 31006 Pamplona, Spain

<sup>b</sup> CIC nanoGUNE Consolider, Tolosa Hiribidea 76, 20018 Donostia, Spain

Received 4 November 2009; received in revised form 29 March 2010; accepted 7 April 2010

Available online 22 April 2010

### Abstract

In this work we provide further advances in the applications of Metamaterial concepts to the classical field of metallic lenses. Some of the limitations that metallic lenses have, such as imperfect matching with free space, can be overcome by Metamaterials, which makes them powerful tools not only in lens field but also in many others. Specifically, our work is devoted to the Extraordinary Transmission Metamaterial because of its low-losses and its potential scaling to any range of the spectrum. Firstly, we explore at the microwave regime the modification of the radiation pattern of a commercial horn antenna when 1 and 4 stacked subwavelength hole arrays are placed as a superstrate. Afterwards, the design of plano- and bi-concave ETM lenses operating at millimetre waves are analysed. Numerical analyses are confirmed by experimental results.

© 2010 Elsevier B.V. All rights reserved.

PACS: 78.70.Gq; 42.15.-i; 42.70.Qs; 42.79.-e

Keywords: Metamaterial; Left-handed medium; Extraordinary transmission; Metallic lens

### 1. Introduction

Lenses are undoubtedly the most widely used optical element for human beings. Examples of its deep penetration into our lives, apart from our own eyes, are glasses, contact lenses, microscopes, telescopes, etc. However, the lenses can also be made to focus electromagnetic waves for other ranges such as microwaves or radio waves with metallic waveguides as Kock developed in the 40 s of the last century [1]. Alike common dielectric lenses, the Kock lenses have a tradeoff between matching and thickness. When the index of refraction is closer to 1, the reflection is lower but the lens needs to be thicker to achieve focusing. On the other hand, the closer the index of refraction is to 0 the thinner the lens will be, but also

the greater the mismatch. This penalty is consequence of the fixed value of the magnetic permeability  $\mu_r = 1$ .

Two recent phenomena have become hot topics in electromagnetism: Metamaterials [2] and Extraordinary Transmission (ET) [3]. The exotic electromagnetic properties arise in both cases as a result of the geometry of their subunit structures—that is, the periodically repeated unit cells such as the classical-used conventional – [4] and complementary-split-ring-resonators [5] – rather than through chemical composition, as it happens with conventional materials. Thus, they are paving the path for very interesting devices with properties that were only guessed at a short time ago.

Metamaterials is a concept that arose when theories of homogenization were applied to periodic structures [4,6]. By this new perspective, macroscopic composites can be defined by effective electromagnetic properties (effective electric permittivity and magnetic permeability, and other constitutive parameters derived from them

\* Corresponding author. Tel.: +34 948169324; fax: +34 648169720.  
E-mail address: [mario@unavarra.es](mailto:mario@unavarra.es) (M. Sorolla).

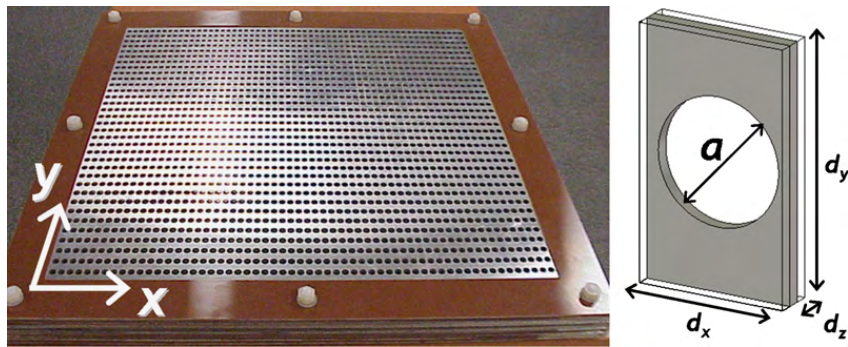


Fig. 1. (Left) Picture of the prototype; (right) unit cell alongside parameters.

such as index of refraction or impedance) which are powerful parameters not only for understanding the underlying physics but also for achieving new designs. This was explored by Shelby et al. to experimentally demonstrate the reality of a Negative Refractive Index (NRI) medium [7] employing a wedge at microwaves [8]. That experiment along with the perfect lens issue [9] were such breakthroughs that this field experienced an unforeseen explosion at the beginning of the 21st century [2,10,11].

On the other hand, periodic arrays of apertures in metallic thin films have been shown to enhance the transmission of electromagnetic waves at wavelengths greater than the aperture diameter. This phenomenon, referred to as ET was first mentioned without further attention by Betzig [12], and investigated into detail by Ebbesen et al. [3] in optics and subsequently demonstrated experimentally at millimetre waves [13] where the surface plasmon polariton responsible of the phenomenon is mimicked by surface waves [14–16].

Recent works have shown that both phenomena can be combined so as to minimize losses [17] on metamaterials structures. It was demonstrated that the close stacking of ET perforated metallic films gives support to backward wave propagation (left-handed propagation is an alternative terminology commonly used) leading to uniaxial effective NRI medium [17–19]. This has made the advantageous combination of concepts [20] an excellent candidate for resonance-based NRI metamaterials at high frequencies such as near-infrared [21] where the classical approach based on split-ring resonators [4] loses the good performance proven at microwaves. It should be noticed that other researchers arrived at similar multilayer structures in parallel and they termed this structure as fishnet because of its resemblance with a fishing mesh [21–23].

Here we extend our previous works on Extraordinary Transmission Metamaterial (ETM) used as planar [24] and curved lens [25,26]. The latter resembles Kock lens, however, the principle of operation is completely differ-

ent since ETM behaves as a NRI medium because of the cut-off regime of operation, whereas Kock lens operates in propagation. In both ETM cases studied in this paper, the hole pattern used has two different in-plane periodicities (the unit cell is rectangular) which improves the filling factor, and thus, the transmittance in real experiments [27]. As a penalty, the ETM is polarization-dependent. In addition to previously published work, we provide retrieved constitutive parameters and an analysis on the frequency-dependent beamwaist (planar lens) and focus (plano- and bi-concave lenses). The planar lens at microwaves is the subject of the first section of this manuscript, whereas the curved lenses designed at millimetre waves are dealt in the next section.

## 2. Microwave planar ETM lens

### 2.1. Design

The subwavelength hole arrays used have the following parameters [24]: hole diameter  $a = 9.25$  mm,  $d_x = 11$  mm,  $d_y = 18.5$  mm, and metal thickness  $w = 1$  mm. The longitudinal lattice constant of the stack is  $d_z = 3$  mm  $\sim 0.145\lambda$  (see Fig. 1). With these parameters and illuminating vertically ( $E_y$ ), that is, along the large periodicity, the ET resonance for one layer falls at 14.5 GHz and the first propagating band of the infinite stack goes from 14.1 to 15.7 GHz, despite the holes are in cut-off regime.

Fig. 2 renders the real and imaginary parts of the effective index of refraction retrieved from S-parameters under normal incidence [28] for several layers (computed with CST Microwave Studio<sup>TM</sup>). In the procedure, the non-physical solutions have been eliminated carefully [28,29]. This approach can be considered valid on this stack because of the subwavelength longitudinal lattice constant. However, notice that the present structure is anisotropic—which could bring interesting consequences like superlensing [30] or subdiffraction [31] to the ETM. However, these issues are beyond the

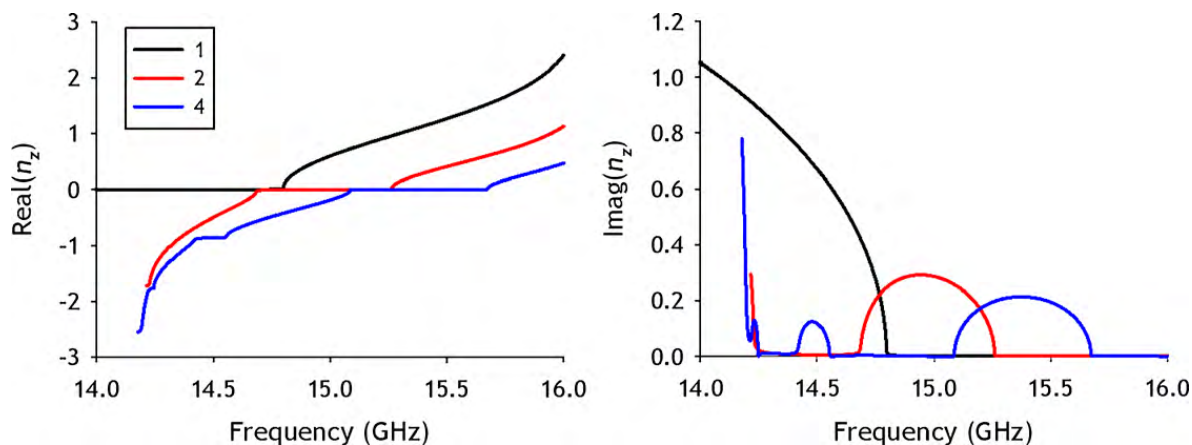


Fig. 2. Real (left) and imaginary (right) parts of the effective index of refraction for 1 (dark curve), 2 (red curve), and 4 perforated plates (blue curve). (For interpretation of the references to color in this figure legend, the reader is referred to the web version of the article.)

scope of the present work – and one of the transverse periodicities is of the order of the wavelength – this is indeed necessary in order to have a displacement current flowing between adjacent layers; see discussion below, – so that the retrieved parameters cannot be interpreted in the same way as in homogeneous continuous and isotropic media. Prominent in this figure is that, unlike the multilayer cases, 1 layer does not present backward propagation (negative index of refraction) (needless to say, the definition of an index of refraction in a 1 layer screen is meaningless because the refractive index is a bulk property. Thus, the value presented here is just a mathematical interpretation of the response of a single layer without real physical meaning). In our formalism, the absence of backward propagation is nothing but the manifestation of the lack of series capacitance in the inverse line equivalent circuit model [17,18,32]. Alternatively, the magnetic response of the multilayer structure is usually explained by some authors [33] following internal surface plasmon polariton interpretation by a loop-like circuit generated via the electric current along each layer and the displacement current flowing from layer to the consecutive one in the direction of the stack. Thus, either the former or the latter interpretation implies that it is mandatory to have a multilayer structure for NRI.

Also, it is worth noting that the effective index of refraction has dependence on the number of stacked layers in such a way that as the number of layers is increased, the frequency bandwidth associated to the backward propagation is wider.

## 2.2. Experimental set-up and results

A numerically controlled drill press has been used to drill several aluminium plates with the hole pattern, see

Fig. 1. The measurements were performed in Labein semi-anechoic chamber with a HP8510C Vector Network Analyser within the frequency range from 11 to 17 GHz.

The aim of the analysis is to characterize the radiation pattern of a set formed by a commercial horn antenna like the EMCO 3115 and an ETM placed in front of it as a lens or superstrate. The antenna EMCO 3115 is placed at 200 mm from the sample and the receiving antenna, also an EMCO 3115, at 1000 mm. The set source and sample are located over a rotary platform so as to allow angular measurements, scanning from  $-90^\circ$  to  $+90^\circ$  with  $1^\circ$  step, see Fig. 3.

Fig. 4 renders the radiation pattern when 1 ET layer is placed in front of the horn antenna at both orthogonal planes E and H (E/H-plane is the plane containing the electric/magnetic field vector and the direction of maximum radiation). H-plane exhibits clearly a broader beamwidth within the ET frequency band than E-plane, whereas the undesired lateral lobes reach higher values in E-plane than in H-plane. Since the periodicity along  $x$  is shorter than along  $y$ , the E-plane is susceptible of higher diffracted modes (grating lobes). In the top panel of Fig. 4 the grating lobes seem to be centred on around  $\pm 70^\circ$ , and they are responsible of the high intensity out of the central zone in the E-plane with respect to H-plane. Finally, for the sample dimensions and the distance of the receiving antenna, the region covered by the ET layer corresponds to an angle close to  $\pm 20^\circ$ , which is in good agreement with the fact that the main beam seems to extend up to this value in both planes of the radiation pattern.

The main features described above do not change much when a 4-layer ETM is introduced, see Fig. 5. The asymmetry is present, with the grating lobes for the E-plane (around  $\pm 80^\circ$  now) as well. However, the

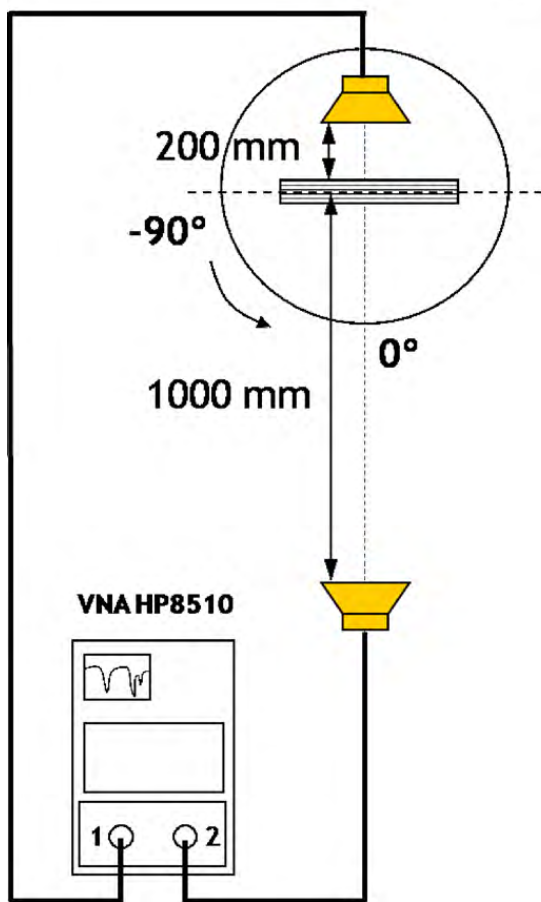


Fig. 3. Sketch of the experimental set-up.

NRI band is better delimited in both planes and the beam within it is slightly narrower than before, as we expected from the fact that the rays impinging obliquely to the structure bend inversely (because of the NRI) and, consequently, the beam suffers less expansion with a consequent increase in the received power.

### 3. Millimetre plano- and bi-concave ETM lens

#### 3.1. Design

The values of the unit cell corresponding to the ETM used for the fabrication of the plano- and bi-concave lenses are:  $d_x = 3$  mm,  $d_y = 5$  mm, hole diameter  $a = 2.5$  mm, and aluminium thickness  $w = 0.5$  mm. The longitudinal lattice constant ( $d_z = 1.5$  mm ( $\sim 0.27\lambda$ )) is chosen so as to achieve a NRI frequency band within our experimental facilities (millimetre waves V-band), see inset Fig. 6.

As it is expected, a similar response of the effective index of refraction retrieved from S-parameter is obtained for this frequency range, see Fig. 7. It has a dependence on the number of illuminated layers and in

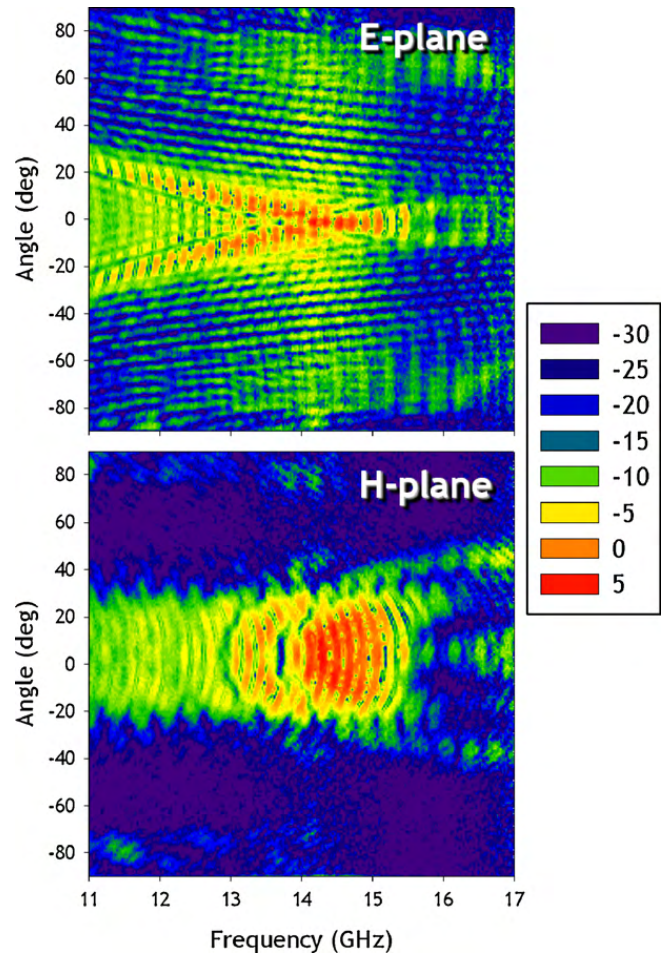


Fig. 4. Radiation pattern as a function of frequency in logarithm scale: E-plane (top) and H-plane (bottom) for 1 ET layer.

the limit, it tends to the index of refraction derived from the dispersion diagram (dotted line).

Once we have the evolution of the effective index of refraction, we can design the curvature of the lens according to Fermat principle/optical length [1,2]. Without loss of generality, we choose as effective index of refraction  $n_z = -1$ . For this value, the profile required for the lens (assuming the other face of the lens is flat) which focuses a plane wave into a point (and the other way around) is a parabola [1,2]. Obviously, by constructing a bi-concave lens, a spherical wave front at the focus is transformed into a spherical wave front with a focus located at two times the focal length from the original focus [26], see Fig. 6. Also, we would arrive at the same conclusions by following geometrical optics [34]. Note that we approach the problem by a stepping profile [25], see Fig. 6, and that the effective index of refraction shown in Fig. 7 cannot accurately define the complete response of the ETM lens because of its anisotropy. Thus, our method based on the effective index of refraction of Fig. 7 is just a first approximation to the problem.

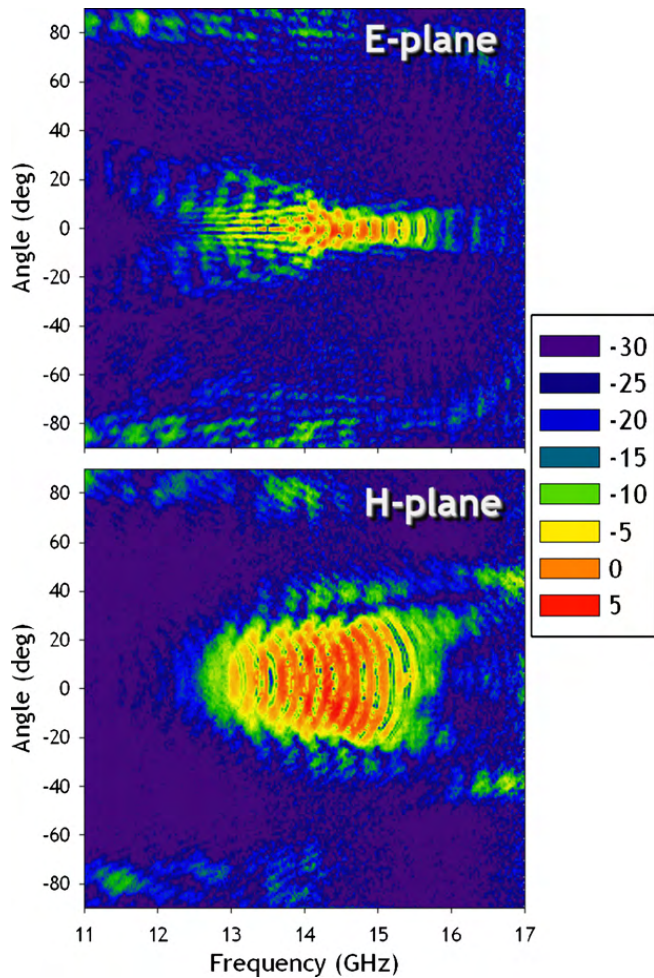


Fig. 5. Radiation pattern as a function of frequency in logarithm scale: E-plane (top) and H-plane (bottom) for 4 ET layer.

### 3.2. Experimental set-up and results

Plano- and bi-concave parabolic prototypes were fabricated by laser-cutting technique in aluminium with the aforementioned parameter values (see schematic in inset

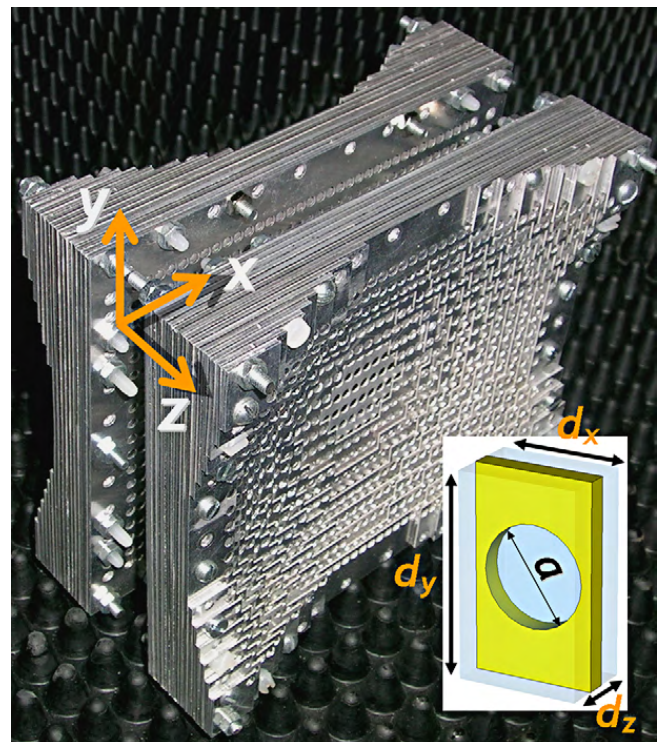


Fig. 6. Picture of two plano-concave metamaterial lenses. Inset: unit cell.

of Fig. 6) and measured with an AB-Millimetre™ Quasioptical Vector Network Analyser.

#### 3.2.1. Frequency dependence of the focus: plano-concave lens

Up to now, we have not analysed the frequency dependence of the focus as a function of the frequency. To do so, numerical calculations have been carried out with CST Microwave Studio™ by using its transient solver and under a plane wave excitation launched towards the flat face of the real plano-concave prototype.

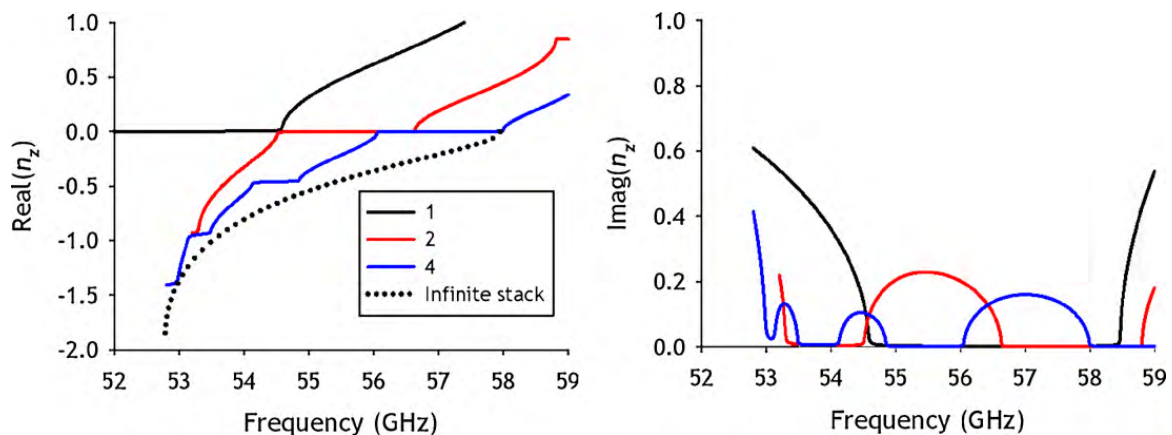


Fig. 7. Real (left) and imaginary (right) parts of the effective index of refraction for 1 (dark curve), 2 (red curve), and 4 perforated plates (blue curve). (For interpretation of the references to color in this figure legend, the reader is referred to the web version of the article.)

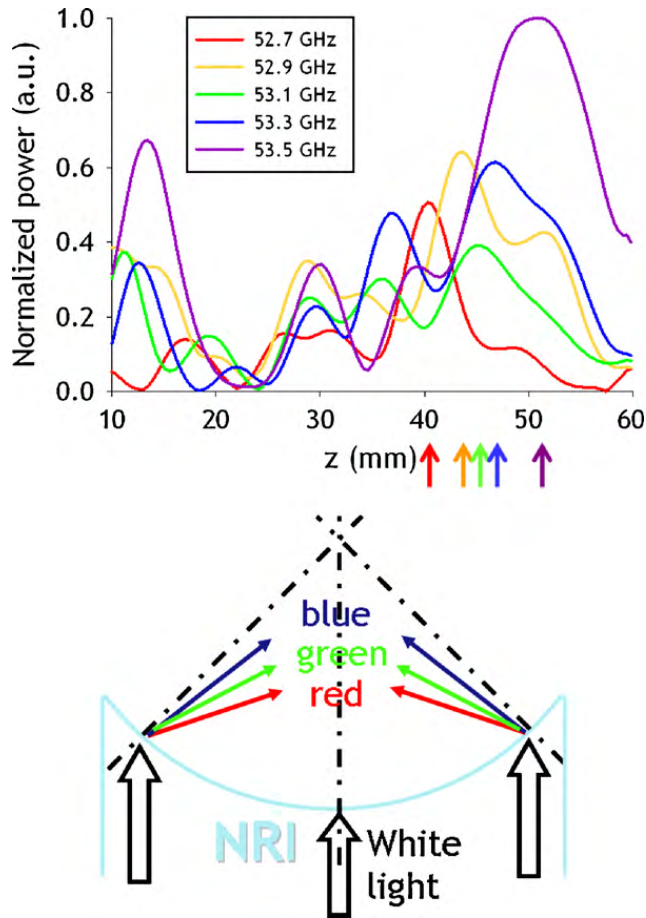


Fig. 8. (Top) Evolution of the focal point along  $z$  as a function of the frequency. To guide the eye, bottom arrows indicate the position of the focus for each frequency. (Bottom) Sketch of ray tracing according to Snell's law.

In Fig. 8a is clearly shown that the focal point moves towards longer distances as the frequency increases. The simple interpretation is the following: the lower (higher) the frequency, the higher (lower) the magnitude of the effective index of refraction; thus, according to Snell's law, the higher (lower) the angle of refraction, see Fig. 8b. In short, from ray tracing, which is just a helpful simplification, at lower frequencies of our NRI band where  $n_z$  is bigger in absolute terms, it is expected that focal point be closer to the lens. The contrary happens when we approach zero (higher frequencies of our NRI band) because then the outgoing ray tends to the normal. Needless to say, the parabola at those frequencies different to  $f_{n=-1}$  is a mere approximation to the optimized lens profile and this is the reason why the focus also suffers a degradation of its magnitude.

### 3.2.2. Characterization of the focus: bi-concave lens

On the other hand, we present subsequently some measurement for the bi-concave lens. The experimen-

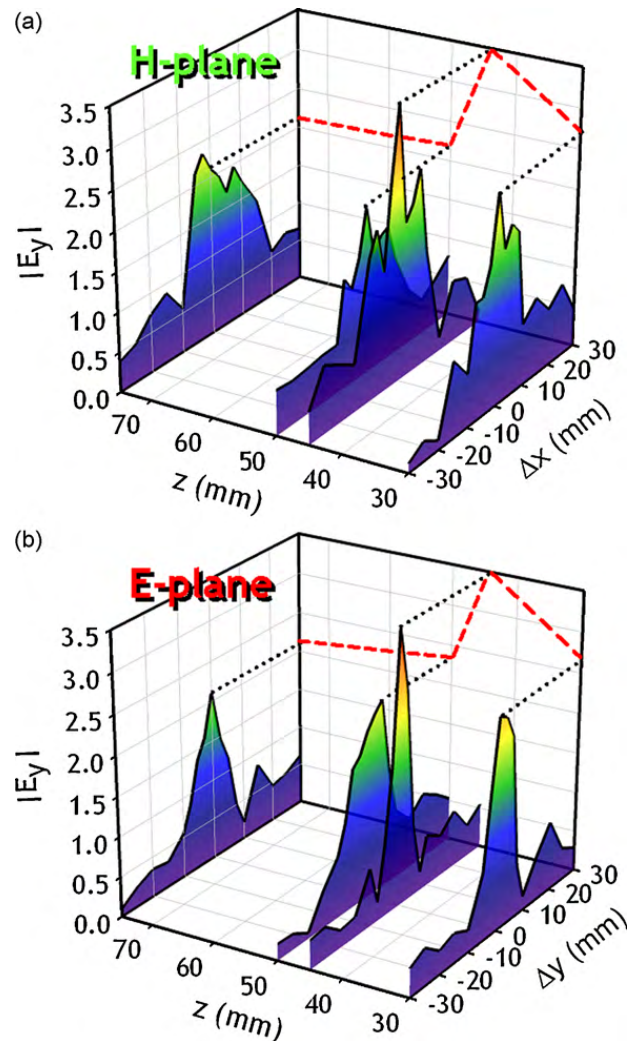


Fig. 9. Experimental electric field intensity  $E_y$  at three different distances from the metamaterial lens: H- (top) and E-plane (bottom).

tal set-up consists of an emitter and a receiver which are open-ended waveguides so as to emulate point source/detector. In the path between both elements the lens is placed and the receiver is manually moved along the image space, while the emitter is fixed to the experimental focal length  $z_{fl} = 45$  mm. Measurement results following this procedure are shown in Fig. 9 at 54.2 GHz (because of non-ideal illumination and working in near-field where evanescent mode cannot be neglected, the experimental frequency, and thus the response of the lens, moves slightly away from simulation [26]). They corroborate the unambiguous focusing effect expected at the image focal point  $z = 45$  mm with an electric magnitude 3.5 times bigger than calibration (magnitude when there is no lens in-between open-ended waveguides).

## 4. Conclusions

Extraordinary Transmission Metamaterials can be applied for beamforming both in flat- and parabolic-lens

configuration. Initial assumptions based on geometrical optics and ray tracing regarding beam compression, lens profile and frequency-dependent focus have been confirmed by numerical, as well as experimental results in microwaves and millimetre waves. It is worth mentioning that simple ideas of ray tracing can be used to understand this lens despite we are at microwaves and millimetre waves and the lens is truly anisotropic [35]. Outstanding of this metamaterial is its potential design in any frequency range of the spectrum. Therefore, unconventional lenses can be foreseen at high frequencies from THz to optics.

### Acknowledgements

We are in debt with J.E. Rodríguez-Seco, E. Perea and I.J. Núñez-Manrique from LABEIN-Tecnalia for their support in the microwave configuration. Also, C. García-Meca and F.J. Rodríguez-Fortuño from Valencia Nanophotonics Technology Center provided a valuable help with respect to the retrieval method.

This work has been supported by the Spanish Government and E.U. FEDER funds under contracts Consolider “Engineering Metamaterials” CSD2008-00066 and TEC2008-06871-C02-01.

### References

- [1] W.E. Kock, Metal-lens antennas, *Proc. IRE* 34 (11) (1946) 828–836.
- [2] L. Solymar, E. Shamonina, *Waves in Metamaterials*, Oxford University Press, New York, 2009.
- [3] T.W. Ebbesen, H.J. Lezec, H. Ghaemi, T. Thio, P.A. Wolf, Extraordinary optical transmission through sub-wavelength hole arrays, *Nature* 391 (6668) (1998) 667–669.
- [4] J.B. Pendry, A.J. Holden, D.J. Robbins, W.J. Stewart, Magnetism from conductors and enhanced nonlinear phenomena, *IEEE Trans. Microw. Theory Technol.* 47 (11) (1999) 2075–2084.
- [5] F. Falcone, T. Lopetegi, M.A.G. Laso, J.D. Baena, J. Bonache, M. Beruete, R. Marqués, F. Martín, M. Sorolla, Babinet principle applied to metasurface and metamaterial design, *Phys. Rev. Lett.* 93 (19) (2004) 1974014.
- [6] J.B. Pendry, A.J. Holden, W.J. Stewart, I. Youngs, Extremely low frequency plasmons in metallic mesostructures, *Phys. Rev. Lett.* 76 (25) (1996) 4773–4776.
- [7] V.G. Veselago, The electrodynamics of substances with simultaneously negative values of  $\epsilon$  and  $\mu$ , *Soviet Phys. Usp.* 10 (4) (1968) 509–514.
- [8] R.A. Shelby, D.R. Smith, S. Schultz, Experimental verification of a negative index of refraction, *Science* 292 (5514) (2001) 77–79.
- [9] J.B. Pendry, Negative refraction makes a perfect lens, *Phys. Rev. Lett.* 85 (18) (2000) 3966–3969.
- [10] S. Tretyakov, *Analytical Modeling in Applied Electromagnetics*, Artech House, Boston, 2003.
- [11] R. Marqués, F. Martín, M. Sorolla, *Metamaterials with Negative Parameters: Theory, Design, and Microwave Applications*, John Wiley and Sons, New York, 2008.
- [12] R.E. Betzig, *Nondestructive optical imaging of surfaces with 500 angstrom resolution*, Doctoral Thesis, 1988.
- [13] M. Beruete, M. Sorolla, I. Campillo, J.S. Dolado, L. Martín-Moreno, J. Bravo-Abad, F.J. García-Vidal, Enhanced millimetre wave transmission through subwavelength hole arrays, *Opt. Lett.* 29 (21) (2004) 2500–2502.
- [14] J.B. Pendry, L. Martín-Moreno, F.J. García-Vidal, Mimicking Surface Plasmons with Structured Surfaces, *Science* 305 (5685) (2004) 847–848.
- [15] D.R. Jackson, A.A. Oliner, T. Zhao, J.T. Williams, The beaming of light at broadside through a subwavelength hole: leaky-wave model and open stopband effect, *Radio Sci.* 40 (2005), RS6S10–112.
- [16] V. Lomakin, E. Michielssen, Enhanced transmission through metallic plates perforated by arrays of subwavelength holes and sandwiched between dielectric slabs, *Phys. Rev. B* 71 (23) (2005) 235117.
- [17] M. Beruete, M. Sorolla, I. Campillo, Left-handed extraordinary optical transmission through a photonic crystal of subwavelength hole arrays, *Opt. Express* 14 (12) (2006) 5445–5455.
- [18] M. Beruete, I. Campillo, M. Navarro-Cía, F. Falcone, M. Sorolla, Molding left- or right-handed metamaterials by stacked cutoff metallic hole arrays, *IEEE Trans. Antennas Propag.* 55 (6) (2007) 1514–1521.
- [19] M. Navarro-Cía, M. Beruete, M. Sorolla, I. Campillo, Negative refraction in a prism made of stacked subwavelength hole arrays, *Opt. Express* 16 (2) (2008) 560–566.
- [20] M. Beruete, M. Navarro-Cía, F. Falcone, I. Campillo, M. Sorolla, Connection between extraordinary transmission and negative refraction in a prism of stacked sub-wavelength hole arrays, *J. Phys. D: Appl. Phys.* 42 (16) (2009) 165504.
- [21] J. Valentine, S. Zhang, T. Zentgraf, E. Ulin-Avila, D.A. Genov, G. Bartal, X. Zhang, Three-dimensional optical metamaterial with a negative refractive index, *Nature* 45 (7211) (2008) 376–379.
- [22] S. Zhang, S.W. Fan, N.C. Panoiu, K.J. Malloy, R.M. Osgood, S.R.J. Brueck, Experimental demonstration of near-infrared negative-index metamaterials, *Phys. Rev. Lett.* 95 (13) (2005) 137404.
- [23] G. Dolling, C. Enkrich, M. Wegener, C.M. Soukoulis, S. Linden, Simultaneous negative phase and group velocity of light in a metamaterial, *Science* 312 (5775) (2006) 892–894.
- [24] M. Beruete, I. Campillo, J.E. Rodríguez-Seco, E. Perea, M. Navarro-Cía, I.J. Núñez-Manrique, M. Sorolla, Enhanced gain by double-periodic stacked subwavelength hole arrays, *IEEE Microw. Wirel. Compon. Lett.* 17 (12) (2007) 831–833.
- [25] M. Beruete, M. Navarro-Cía, M. Sorolla, I. Campillo, Planoconcave lens by negative refraction of stacked subwavelength hole arrays, *Opt. Express* 16 (13) (2008) 9677–9683.
- [26] M. Navarro-Cía, M. Beruete, M. Sorolla, I. Campillo, Converging biconcave metallic lens by double-negative extraordinary transmission metamaterial, *Appl. Phys. Lett.* 94 (14) (2009) 144107.
- [27] M. Beruete, M. Sorolla, M. Navarro-Cía, F. Falcone, I. Campillo, V. Lomakin, Extraordinary transmission and left-handed propagation in miniaturized stacks of doubly periodic subwavelength hole arrays, *Opt. Express* 15 (3) (2007) 1107–1114.
- [28] X. Chen, T.M. Grzegorzczak, B.-I. Wu, J. Pacheco, J.A. Kong Jr, Robust method to retrieve the constitutive effective parameters of metamaterials, *Phys. Rev. E* 70 (1) (2004) 016608.
- [29] Y. Hao, R. Mittra, *FDTD Modeling of Metamaterials—Theory and Applications*, Artech House, Norwood, 2009.

- [30] N.-H. Shen, S. Foteinopoulou, M. Kafesaki, T. Koschny, E. Ozbay, E.N. Economou, C.M. Soukoulis, Compact planar far-field superlens based on anisotropic left-handed metamaterials, *Phys. Rev. B* 80 (11) (2009) 115123.
- [31] Y. Xiong, Z. Liu, X. Zhang, Projecting deep-subwavelength patterns from diffraction-limited masks using metal-dielectric multilayers, *Appl. Phys. Lett.* 93 (11) (2008) 111116.
- [32] M. Beruete, M. Navarro-Cía, I. Campillo, F. Falcone, I. Arnedo, M. Sorolla, Parametrical study of left-handed or right-handed propagation by stacking hole arrays, *Opt. Quant. Electron.* 39 (4–6) (2007) 285–293.
- [33] R. Ortuño, C. Garcí-a-Meca, F.J. Rodríguez-Fortuño, J. Martí, A. Martínez, Role of surface plasmon polaritons on optical transmission through double layer metallic hole arrays, *Phys. Rev. B* 79 (7) (2009) 075425.
- [34] S. Cornbleet, *Microwave Optics—The Optics of Microwave Antenna Design*, Academic Press, 1976.
- [35] M. Beruete, M. Navarro-Cía, M. Sorolla, I. Campillo, Negative refraction through an extraordinary transmission left-handed metamaterial slab, *Phys. Rev. B* 79 (19) (2009) 195107.